Journal of Dermatological Science 93 (2019) 101–108

Contents lists available at ScienceDirect

Journal of Dermatological Science

journal homepage: www.jdsjournal.com

Original Article

Atypical protein kinase C isoforms differentially regulate directional keratinocyte migration during wound healing

Natsuko Noguchi[a], Tomonori Hirose[b], Tomoko Suzuki[a], Masami Kagaya[a], Kazuhiro Chida[c], Shigeo Ohno[b], Motomu Manabe[a], Shin-Ichi Osada[a,*]

[a] Department of Dermatology & Plastic Surgery, Akita University Graduate School of Medicine, Akita, Japan
[b] Department of Molecular Biology, Yokohama City University Graduate School of Medical Science, Yokohama, Japan
[c] Department of Animal Resource Sciences, Graduate School of Agricultural and Life Sciences, The University of Tokyo, Tokyo, Japan

ARTICLE INFO

Article history:
Received 2 November 2018
Received in revised form 12 December 2018
Accepted 3 January 2019

Keywords:
Cell polarity
aPKC
Wound healing
Cell migration

ABSTRACT

Background: The epidermis possesses regenerative properties that become apparent only after wounding. Atypical protein kinase C (aPKC) isoforms aPKCζ and aPKCλ form a ternary complex with Par3 and Par6, and play crucial roles in establishing and maintaining epithelial cell polarity. The epidermal loss of aPKCλ results in progressive depletion of hair follicle stem cells. However, it is unclear whether aPKCs have equivalent activities in epidermal regeneration.
Objectives: To clarify functional differences between aPKCζ and aPKCλ in cutaneous wound healing.
Methods: We compared cutaneous wound healing processes in vivo using mutant mice with genetic deletion of each aPKC isoform. We also analyzed functional differences between aPKCζ and aPKCλ in cell proliferation, directional cell migration, and formation of microtubules in vitro using primary keratinocytes established from each mutant mouse.
Results: Wound healing was significantly retarded in epidermis-specific aPKCλ knockout mice. In aPKCλ-deleted keratinocytes, the correct orientation of cell protrusions toward the wound was disrupted through the destabilization of Par6β. The elongation of stabilized β-tubulin was also deteriorated in aPKCλ-deleted keratinocytes, leading to defects in cell spreading. Conversely, wound healing and directional cell migration in aPKCζ-deleted mice were comparable to those in their control littermates.
Conclusions: aPKCs are not functionally equivalent; aPKCλ, but not aPKCζ, plays a primary role in cutaneous wound healing.

1. Introduction

The mammalian epidermis has a polarized and stratified structure. Atypical protein kinase C (aPKC) is a crucial component of the aPKC/Par3/Par6 ternary complex, which is localized at the apical domain of epithelial cells and functions as a determinant of cell polarity [1,2]. The aPKC-Par complex presumably interacts with the spindle orientation machinery composed of Gαi3, LGN, mInsc, NuMA, and dynactin [3,4] and is implicated in Notch signaling-mediated epidermal stratification, differentiation, and barrier formation [3].

Mammals possess two aPKC isoforms, aPKCζ and aPKCλ, which are expressed in the epidermal basal layer [5]. We and another group generated conditional epidermis-specific aPKCλ-knockout (aPKCλ cKO) mice and found that these mutant mice displayed progressive hair loss and gradual depletion of the hair follicle stem cell (HFSC) population with age [6,7].

Wound healing assay represents a classical and useful experimental system to investigate skin regeneration, wherein several distinct progenitor populations in the hair follicle (HF) mobilize to the wound area and contribute to re-epithelialization [8,9]. Keratin 15 (K15)-positive progenitor cells located in the bulge/secondary hair germ region of the HF are transiently involved in re-epithelialization [10], whereas Lrig1+ cells originating from the pilosebaceous compartment, Lgr6+ cells in the isthmus, and Gli1+ cells in the upper bulge region contribute to long-term epidermal healing [11–14]. Given these findings, it is important to investigate the wound healing processes in aPKCλ cKO mice, in which the HFSCs are mislocalized and gradually depleted [6,7].

Abbreviations: aPKC, atypical protein kinase C; HF, hair follicle; HFSC, hair follicle stem cell.

* Corresponding author at: Department of Dermatology & Plastic Surgery, Akita University Graduate School of Medicine, Akita 010-8543, Japan.
E-mail address: osada0130@gipc.akita-u.ac.jp (S.-I. Osada).

https://doi.org/10.1016/j.jdermsci.2019.01.001
0923-1811/

Cell polarization and directional cell migration are crucial steps in wound healing, and aPKCs have been implicated in these processes [15]. In rodent primary astrocytes and embryonic fibroblasts, the Cdc42/Par/aPKC complex and the noncanonical Wnt signal transduction pathways cooperate to promote cell polarity [16–18]. These reports mainly examined the role of the aPKCζ isoform in directional cell migration during wound healing. For example, in a scratch-wound assay on a monolayer of rat astrocytes, aPKCζ is strongly activated and associates with Par6 and Cdc42 [17]. As for keratinocytes, TIAM1, which is a Rac exchange factor and associates with Par3 and aPKCζ at the leading edge of keratinocytes, regulates cell migration [19]. However, these results did not exclude the possibility that aPKCλ is involved in directional cell migration. Remarkably, in contrast to aPKCλ cKO mice, no skin phenotypes were reported in aPKCζ KO mice [20]. Thus, it remains unclear whether aPKCζ and aPKCλ are functionally equivalent in directional cell migration during wound healing. Here, we aimed to answer these questions using mutant mice with genetic deletion of each aPKC isoform to assess their roles in cutaneous wound healing in vivo.

2. Materials and methods

2.1. Animals

Generation of aPKCζ knockout (aPKCζ KO, *Prkcz*$^{-/-}$) mice and conditional epidermis-specific aPKCλ-knockout (aPKCλ cKO, *keratin 5-Cre; aPKCλ*$^{\Delta E5/\Delta E5}$) mice is described elsewhere [7,21]. *Prkcz*$^{+/-}$ and *keratin 5-Cre; aPKCλ*$^{\Delta E5/+}$ mice were used as controls. All animal experiments were approved by the animal research committee of Akita University School of Medicine (No. 26-1-84).

2.2. Antibodies

Primary antibodies used in this study and their working dilutions in immunohistochemistry were as follows: keratin 14 (1:1000, Covance, Princeton, NJ, USA), keratin 15 (1:50, Thermo Fisher Scientific, Waltham, MA, USA), Par3 (BD Biosciences, Franklin Lakes, NJ, USA), Par6β (Santa Cruz Biotechnology, Santa Cruz, CA, USA), β-catenin (BD Biosciences), GSK3β (BD Biosciences), phospho-GSK3β (Cell Signaling Technology, Danvers, MA, USA), Numb (Cell Signaling Technology), phospho-Numb (Cell Signaling Technology), vinculin (1:1000, Signa, Saint Luis, MO, USA), GM130 (1:500, BD Biosciences), β-tubulin (1:100, Cell Signaling Technology), Acti-stain 488 fluorescent phalloidin (100 nM, Cytoskeleton, Denver, CO, USA), and anti-α-actinin (1:100, Cell Signaling Technology).

2.3. Wound healing and morphometric analysis of wound closure

Full-thickness wounds (2.25 cm^2; 1.5 cm × 1.5 cm) were generated on the mid-back of 7–8-week-old mice. Wounds were photographed using a scale, and wound areas were calculated using Image J Software (National Institutes of Health, Bethesda, MD, USA). Histology and immunohistochemistry were performed as described previously [7].

2.4. Golgi reorientation

Golgi reorientation was measured as previously described [17]. Briefly, the cells in the front 1–2 rows facing the wound, in which the Golgi was within the 120-degree sector, were regarded as positive.

2.5. In vitro wound healing assay and morphometric analysis

Skin specimens removed from euthanized newborn mice were incubated in Dulbecco's modified Eagle's medium (DMEM; Life Technologies, Carlsbad, CA, USA) supplemented with 10% fetal bovine serum (FBS) and 2 mg/ml dispase (Invitrogen, Waltham, MA, USA) at 4 °C overnight. After peeling off the dermis, the epidermis was further incubated in 0.25% trypsin/0.02% ethylenediaminetetraacetic acid (EDTA) (Life Technologies) for 15 min at 37 °C. Keratinocytes were seeded at a density of 8×10^5 cells per well in a 12-well culture plate on a coverslip coated with type I collagen (Nitta Gelatin Inc., Osaka, Japan) and incubated in keratinocyte growth medium (KGM; Kurabo, Osaka, Japan) supplemented with bovine pituitary extract (BPE) and human epidermal growth factor (hEGF) until reaching confluence. After the medium was replaced with KGM without BPE and hEGF, the cells were further incubated for 24 h, and an artificial linear wound was created using a 200-μl pipette tip. Plates were fixed with methanol at 24, and 48 h after wounding and stained with 0.5% crystal violet in 50% methanol.

After photographs of five independent fields were taken for each well at 0, 24, and 48 h following wounding, wound areas were outlined using Image J software, and the outlined areas were calculated. The percent wound confluence was calculated using the following equation:

$$\%\ \text{wound confluence} = [(A - B) \times 100]/A$$

where A is the wound area of the initial scratch wound, and B is the wound area of the scratch wound 24 or 48 h after wounding.

2.6. Cell proliferation assay

Primary keratinocytes prepared as described above were seeded at a density of 1×10^5 cells per well in triplicate in a 24-well plate. On the day of the assay, the medium was replaced with 0.5 ml of DMEM without FBS containing 10% Alamar blue (Invitrogen). After 4 h of incubation, 0.1 ml of the medium from each well was transferred to a 96-well microplate. Fluorescence (540 nm excitation, 590 nm emission) was measured on a Fluoroskan Ascent Microplate Fluorometer (Thermo Electron Oy, Waltham, MA, USA) on days 0, 2, 4, and 6.

2.7. Western blot analysis

Epidermal samples were homogenized in 1× RIPA buffer (50 mM Tris–HCl pH 7.5, 1% NP-40, 0.5% sodium deoxycholate, 0.1% SDS, 150 mM NaCl, 1 mM EDTA) containing cOmplete Mini protease inhibitor cocktail (Roche, Mannheim, Germany) and PhosSTOP phosphatase inhibitor cocktail (Roche) and microcentrifuged. The supernatants were subjected to sodium dodecyl sulfate -polyacrylamide gel electrophoresis and electrotransferred to a polyvinylidene difluoride membrane, which was then soaked in 5% non-fat milk in 1 × phosphate buffered saline. The membrane was incubated with primary antibodies and then with horseradish peroxidase-conjugated secondary antibody (GE Healthcare Life Sciences, Marlborough, MA, USA). Detection was carried out using a Clarity Western ECL substrate (Bio-Rad, Hercules, CA, USA).

2.8. Quantification and statistical analysis

Data are presented as the mean ± standard deviation (SD). The significance of differences between groups for quantitative data was determined using the unpaired two-tailed Student's *t*-test in Microsoft Excel 2011 (Microsoft, Redmond, WA, USA).

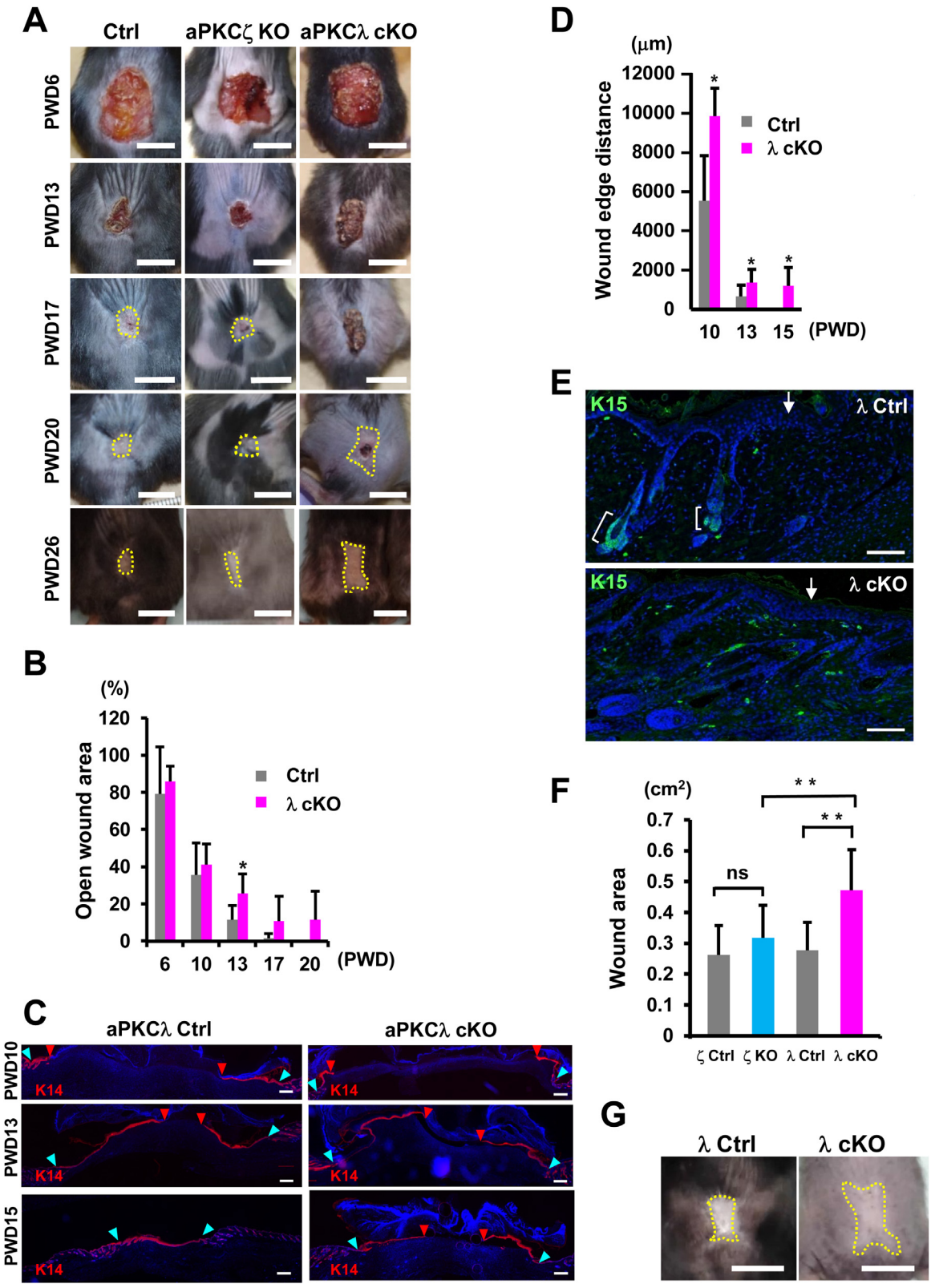

Fig. 1. Retarded wound healing in epidermis-specific aPKCλ-knockout mice. (A) Representative macroscopic views of the wound healing processes in control (left column, n = 10), aPKCζ KO mice (middle column, n = 5), and aPKCλ cKO mice (right column, n = 10). Post-wound days (PWD) are indicated. Yellow dotted lines indicate wound scars. Bar = 1 cm. (B) Percent Open wound area measured at indicated post-wound days. The ratio was expressed as the wound area at the indicated PWD divided by the initial wound area. $^{*}p < 0.01$. (C) Anti-K14 antibody immunostaining of the sections of the wound at the indicated PWDs. Bar = 500 μm. Blue and red triangles indicate the original and healing wound edges, respectively. (D) Quantification of the distance between the healing wound edges at the indicated PWDs in control (10 sections at PWD10, 16 sections at PWD 13, and 13 sections at PWD 15) and aPKCλ cKO (7 sections at PWD10, 14 sections at PWD 13, and 12 sections at PWD 15) mice. Data are presented as the mean ± SD. $^{*}p < 0.01$. (E) Immunohistochemistry of the regions adjacent to the wound in control and aPKCλ cKO mice at PWD 17 using an anti-K15 antibody. White arrows, the normal skin–wound border. Brackets, K15-positive HFSCs. Bar = 100 μm. (F) Quantification of the wound area at PWD 26 in the aPKCζ control (n = 12), aPKCζ KO (n = 12), aPKCλ control (n = 23), and aPKCλ cKO (n = 22) mice. ns, not significant. $^{**}p < 0.001$. (G) Macroscopic views of wound scars in control and aPKCλ cKO mice at PWD 180. Bar = 1 cm.

3. Results

3.1. aPKC isoforms differentially contribute to integumentary structure development

Two isoforms of aPKC, aPKCζ and aPKCλ, are expressed in the epidermis [5]. Although aPKCλ cKO mice are known to show progressive hair loss [6,7], the precise role of aPKCζ in the epidermis and the adnexal structures has not yet been fully elucidated. Therefore, we first examined integumentary structure development in aPKCζ KO mice [21]. The integumentary structures of aPKCζ KO mice were grossly and histologically indistinguishable from those of control mice (Fig. S1A–C). Moreover, in contrast to aPKCλ cKO mice, where the expression of HFSC markers was diminished and/or mislocalized [6,7], HFSC markers were normally expressed, and the number of HFSCs was not changed in aPKCζ KO mice (Fig. S2A–C). These results indicated that aPKCζ is dispensable for epidermal and adnexal development.

3.2. Cutaneous wound healing retardation in aPKC λ cKO mice

Because K15-positive HFSCs, which are transiently involved in re-epithelialization during wound healing [9,10], are gradually depleted in aPKCλ cKO mice [6,7], we hypothesized that wound healing processes are impaired in the mutant mice. To

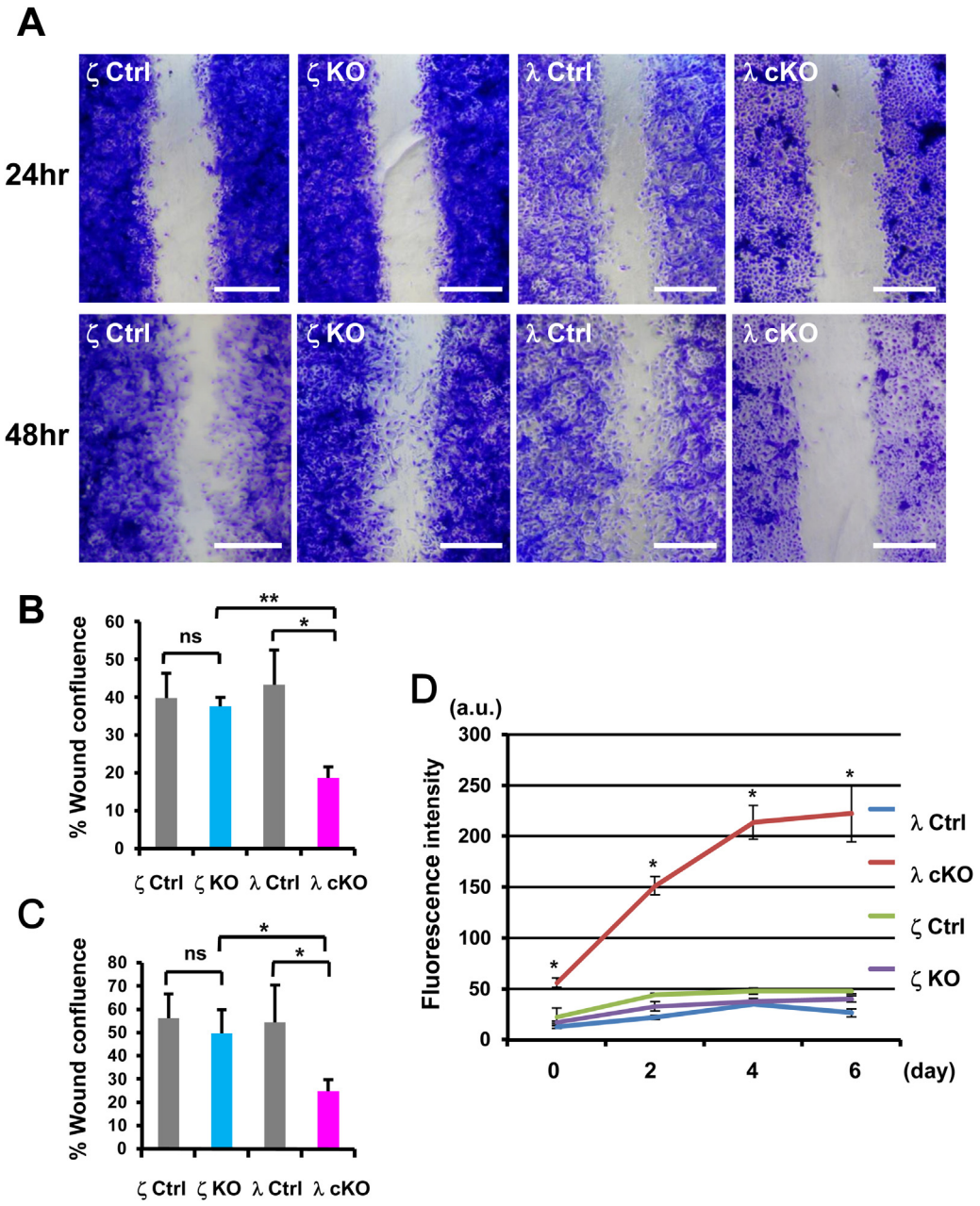

Fig. 2. Impaired directional cell migration in aPKCλ-deleted keratinocytes. (A) Scratch wound healing assay on a monolayer of primary keratinocytes from the aPKCζ control (n = 5 for 24 h, n = 3 for 48 h), aPKCζ KO (n = 2 for 24 h, n = 3 for 48 h), aPKCλ control (n = 3 for 24 h, n = 5 for 48 h), and aPKCλ cKO mice (n = 5 for 24 h, n = 11 for 48 h). The cells were stained 24 h (upper panels) and 48 h (lower panels) after wounding using 0.5% crystal violet. Representative images of the wound areas for each genotype are shown. Bar = 500 μm. (**B**) Percent wound confluence 24 h after wounding. Data are presented as the mean ± SD. $^{*}p < 0.1$, $^{**}p < 0.05$. (C) Percent wound confluence 48 h after wounding. $^{*}p < 0.05$. (D) Cell proliferation assay in cultured aPKCζ control, aPKCζ-deleted, aPKCλ control, and aPKCλ-deleted keratinocytes at 0, 2, 4, and 6 days. Each experiment was performed in triplicate. Representative data for three independent experiments are shown. a.u., arbitrary unit. $^{*}p < 0.05$.

examine this possibility, a 2.25 cm^2 (1.5 cm × 1.5 cm) full-thickness wound was created on the mid-back of 7–8-week-old control and mutant mice for each aPKC isoform. Because aPKCλ cKO mice show growth retardation and surgical insult on younger mice resulted in early death, we created the wounds in 7-8-week-old mice.

At post-wound day (PWD) 6, no clear difference was observed in wound closure between control and aPKCλ cKO mice (Fig. 1A). However, wound healing was noticeably retarded at PWD 13 in aPKCλ cKO mice (Fig. 1B). In control and aPKCζ KO mice, scab shedding and re-epithelialization were completed at around PWD 17 and PWD 20, respectively. However, in aPKCλ cKO mice, these wound healing processes were significantly delayed (Fig. 1A). Keratin 14 immunostaining revealed that the wound was re-epithelialized in aPKCλ control mice at PWD 15 below the scab, whereas re-epithelialization was not completed in the aPKCλ cKO mice at this time-point (Fig. 1C, D). As expected, K15+ bulge stem cells were diminished in the peri-wound HFs of aPKCλ cKO mice (Fig. 1E). Wound contraction was also severely impaired in aPKCλ cKO mice. The average wound area at PWD 26 was about 1.7-fold larger in aPKCλ cKO mice (0.47 ± 0.13 cm^2) than in λ control (0.28 ± 0.09 cm^2), ζ control (0.26 ± 0.09 cm^2), and aPKCζ KO mice (0.32 ± 0.10 cm^2) (Fig. 1F). The wound scar on the back of aPKCλ cKO mice showed no considerable contraction even at PWD 180 (Fig. 1G). These results suggest that the delayed wound healing in aPKCλ cKO mice results from defects in epidermal cell migration and wound contraction.

3.3. The loss of aPKCλ impaired keratinocyte migration

We next performed an in vitro scratch wound assay to examine whether the defect in wound closure in aPKCλ cKO mice does indeed result from defective migratory activity of keratinocytes. A scratch wound was created on a primary keratinocyte monolayer prepared from control and each of the aPKC KO mice. Wound confluence was markedly decreased in aPKCλ-deleted keratinocytes at both 24 and 48 h after scratching compared to that in controls and aPKCζ-deleted keratinocytes (Fig. 2A–C). The percent wound confluence after 24 h was $39.9 \pm 6.57\%$ in ζ control, $37.6 \pm 2.44\%$ in aPKCζ KO, $43.3 \pm 9.17\%$ in λ control, and $18.8 \pm 2.84\%$ in aPKCλ cKO mice; it was $56.2 \pm 10.5\%$ in ζ control, $49.8 \pm 10.03\%$ in aPKCζ KO, $54.4 \pm 16.0\%$ in λ control, and $24.8 \pm 5.0\%$ in aPKCλ cKO mice after 48 h.

The impaired wound confluence in aPKCλ-deleted keratinocytes could be explained by defects in cell proliferation or migration. As shown in Fig. 2D, primary keratinocytes from aPKCλ cKO mice showed markedly higher cell proliferation activity than controls and aPKCζ-deleted keratinocytes. These results suggest that delayed wound healing in aPKCλ cKO mice was not due to impaired cell proliferation in the epidermis.

3.4. Directional cell migration was impaired in aPKCλ-deleted keratinocytes

We next examined whether the directional cell migration toward the wound was affected in aPKCλ-deleted keratinocytes. A major

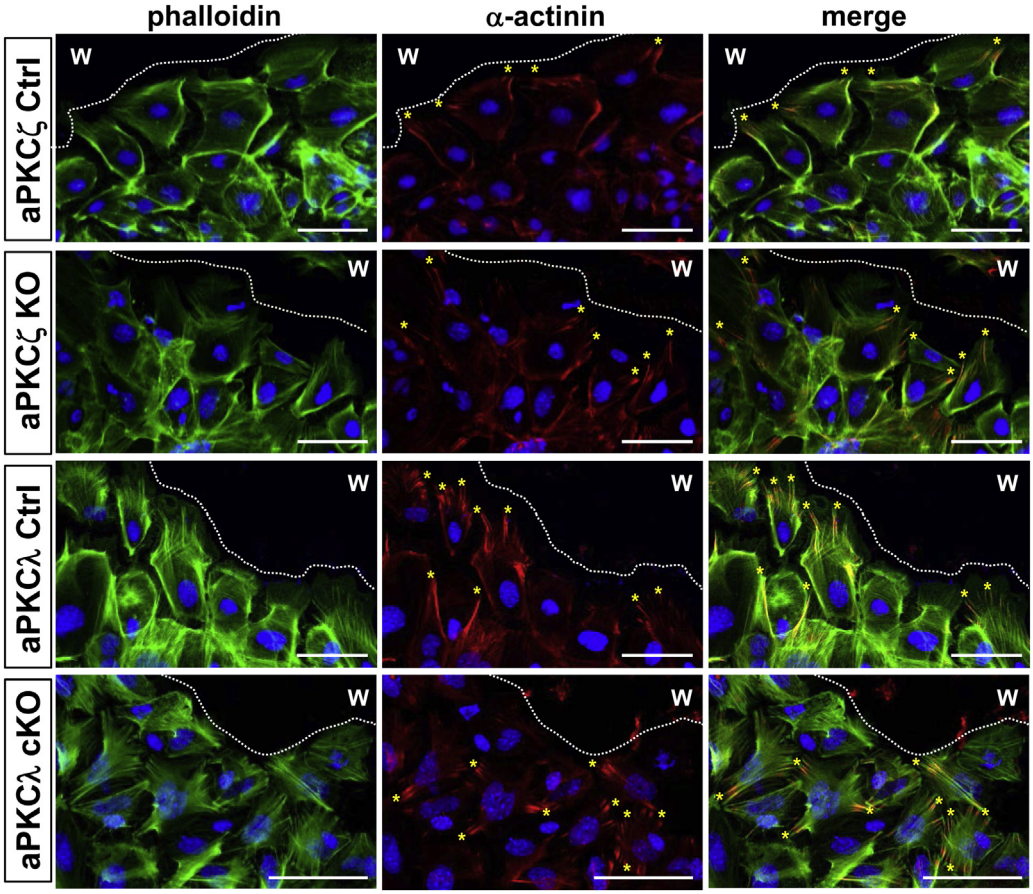

Fig. 3. Randomization of the direction of cellular protrusions in aPKCλ-deleted keratinocytes. Closer views of wound-edge primary keratinocytes from aPKCζ control (n = 3), aPKCζ-deleted (n = 3), aPKCλ control (n = 3), and aPKCλ-deleted (n = 5) keratinocytes stained with phalloidin (green) and α-actinin (red) 48 h after wounding. Representative data are shown. Nuclei were counterstained with DAPI. Dotted white lines indicate the scratched wound (w) borders. Bar = 10 μm. Yellow asterisks indicate the direction of actin protrusions. Note that the scale bars in aPKCλ-deleted keratinocytes are longer than those in the control and aPKCζ-deleted keratinocytes.

consequence of disruption of the monolayer is to induce polarity in cells proximal to the scratch. One aspect of polarization is the formation of actin-rich protrusions, specifically at the front of the cell [22]. Because α-actinins, actin cross-linking proteins, localize to the lamellipodial extension of motile cells [23,24], we used α-actinin as a marker for the leading edge. In controls and aPKCζ-deleted keratinocytes, wound-edge keratinocytes extended unidirectional cellular protrusions toward the scratch wound, whereas the direction of cellular protrusions was random in aPKCλ-deleted keratinocytes (Fig. 3). These results suggest that aPKCλ, but not aPKCζ, regulates directional cell migration during cutaneous wound healing.

3.5. The epidermal loss of aPKC λ destabilized Par6β

Another aspect of polarization involves the microtubule cytoskeleton and can be visualized as reorientation of the Golgi [17]. As shown in Fig. 4A, Golgi reorientation was also disturbed in aPKCλ-deleted migrating keratinocytes. In aPKCζ control, aPKCζ-deleted, and aPKCλ control, approximately 45% of migrating primary keratinocytes facing the wound had the Golgi in the forward-facing 120-degree sector, whereas this percentage was significantly decreased to approximately 10% in aPKCλ-deleted keratinocytes (Fig. 4B).

To examine the mechanisms underlying the observed cell migration defects in aPKCλ-deleted keratinocytes, we examined the expression of Par3, Par6β, and components of the Wnt signaling pathway at the protein level. As shown in Fig. 4C, the expression level of Par3 was unchanged in the aPKCλ-deleted epidermis, whereas that of Par6β was significantly decreased. Concomitantly, the level of phosphorylated GSK-3β was increased. Although in HeLa cells suppressed expression of both aPKCζ and aPKCλ by siRNAs reduced the phosphorylation of Numb [25], the level of phosphorylated Numb was unchanged in aPKCλ-deleted epidermis. The expression levels of Par3 and Par6β were unchanged in the

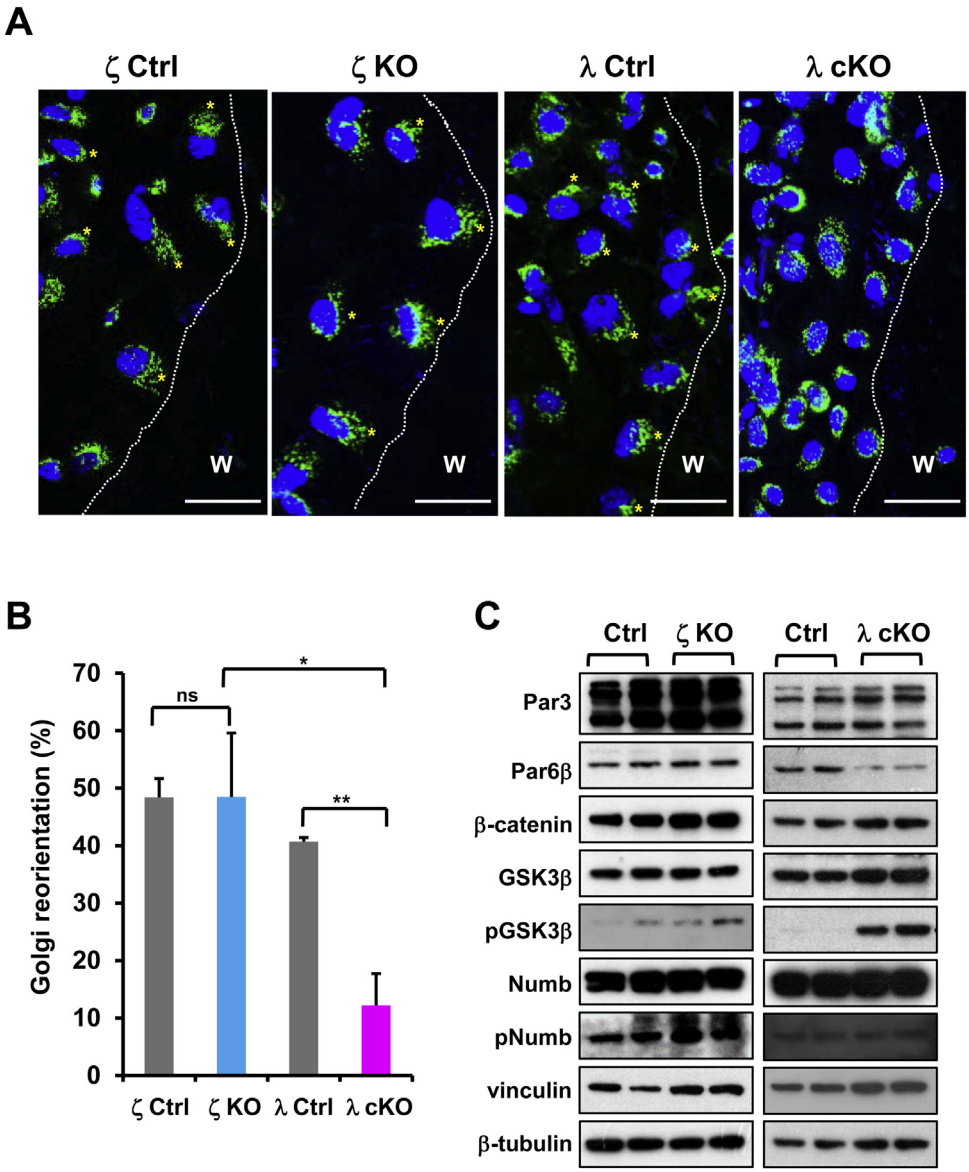

Fig. 4. The loss of epidermal aPKCλ destabilized Par6β. (A) Representative images of the Golgi reorientation of the migrating keratinocytes facing the wound. The Golgi was immunostained with an anti-GM130 antibody. Genotypes are indicated. Bar = 50 μm. Yellow asterisks indicate the Golgi within the 120-degree sector. (B) Quantification of the Golgi reorientation. At least 200 cells of each genotype (n = 3) were examined. $^{*}p < 0.05$, $^{**}p < 0.001$. (C) Immunoblot analysis of the newborn epidermis from aPKCζ control, aPKC ζ KO, aPKCλ control, and aPKC λ cKO mice with indicated antibodies. The phosphorylated forms of GSK3β and Numb are indicated by the prefix 'p'. The levels of β-tubulin were used as a loading control.

aPKCζ-deleted epidermis. These results suggested that aPKCλ, but not aPKCζ, regulates directional cell migration through the stabilization of Par6β and the phosphorylation status of GSK-3β. Because the interaction between Par6 and aPKC is mediated by the catalytic domain of aPKCs and the PDZ domain of PAR6 [26,27], the lack of aPKCλ may destabilize Par6β.

3.6. The loss of epidermal aPKCλ affected the elongation of stabilized β-tubulin

Closer inspection of wound-edge keratinocytes revealed that cell spreading was also impaired in aPKCλ-deleted keratinocytes (Fig. 5A). Control and aPKCζ-deleted wound-edge keratinocytes formed well-developed lamellipodia towards the wound compared to aPKCλ-deleted keratinocytes. Morphometric analysis of wound-edge keratinocytes further revealed that the average cell areas for aPKCζ control, aPKCζ-deleted, aPKCλ control, and aPKCλ-deleted keratinocytes were $3{,}913 \pm 1{,}627\ \mu m^2$, $3{,}840 \pm 1{,}391\ \mu m^2$, $2{,}775 \pm 1{,}503\ \mu m^2$, and $1{,}485 \pm 905\ \mu m^2$, respectively (Fig. 5B).

The defects in the cell spreading of aPKCλ-deleted keratinocytes can be explained by the defects in cell-substrate adhesion. The expression of vinculin, an adaptor protein controlling cell-substrate adhesion signaling, was unchanged in aPKCλ- and aPKCζ-deleted epidermis (Fig. 4C). However, immunostaining with an anti-β-tubulin antibody revealed that the extension of stabilized β-tubulin microtubules was perturbed in aPKCλ-deleted keratinocytes (Fig. 5C), suggesting that the defects in the cell spreading of aPKCλ-deleted keratinocytes could be explained by this impairment of microtubule extension.

4. Discussion

Here, we revealed that two aPKC isoforms expressed in the epidermis are differentially implicated in cutaneous wound healing. Previous in vitro studies indicated that aPKCζ controls directional cell migration during wound healing [16–18]. However, functional differences between aPKCζ and aPKCλ in wound healing has not been directly addressed except that overexpression of aPKCζ, but not aPKCλ, inhibits astrocyte polarization [17]. Using genetically deleted mice for each aPKC isoform, we found that aPKCλ plays a primary role in cutaneous wound healing in vivo. We also demonstrated that aPKCλ regulates the direction of cellular protrusions of migrating keratinocytes during wound healing and that the protein levels of Par6β are destabilized in aPKCλ-deleted, but not in aPKCζ-deleted keratinocytes. This is consistent with the previous observation that aPKCλ knockdown in MDCK cells decreased the protein level of Par6β [28].

In scratch-induced astrocyte migration the Cdc42/Par6/aPKCζ pathway phosphorylates glycogen synthase kinase-3β (GSK-3β) to inhibit its catalytic activity and the phosphorylation of GSK-3β leads to its dissociation from aPKCζ [18]. In contrast, we showed that the GSK-3β phosphorylation level was increased in the absence of aPKCλ. Although we currently do not know how the phosphorylation of GSK-3β was upregulated in the aPKCλ-deleted keratinocytes, the loss of aPKCλ may activate other kinase(s), inactivate phosphatase(s), or release the inhibitory effects of GSK-3β–interacting proteins. Increased phosphorylated GSK-3β may lose its accessibility to aPKCζ, which further promotes the randomized migration direction of aPKCλ-deleted keratinocytes.

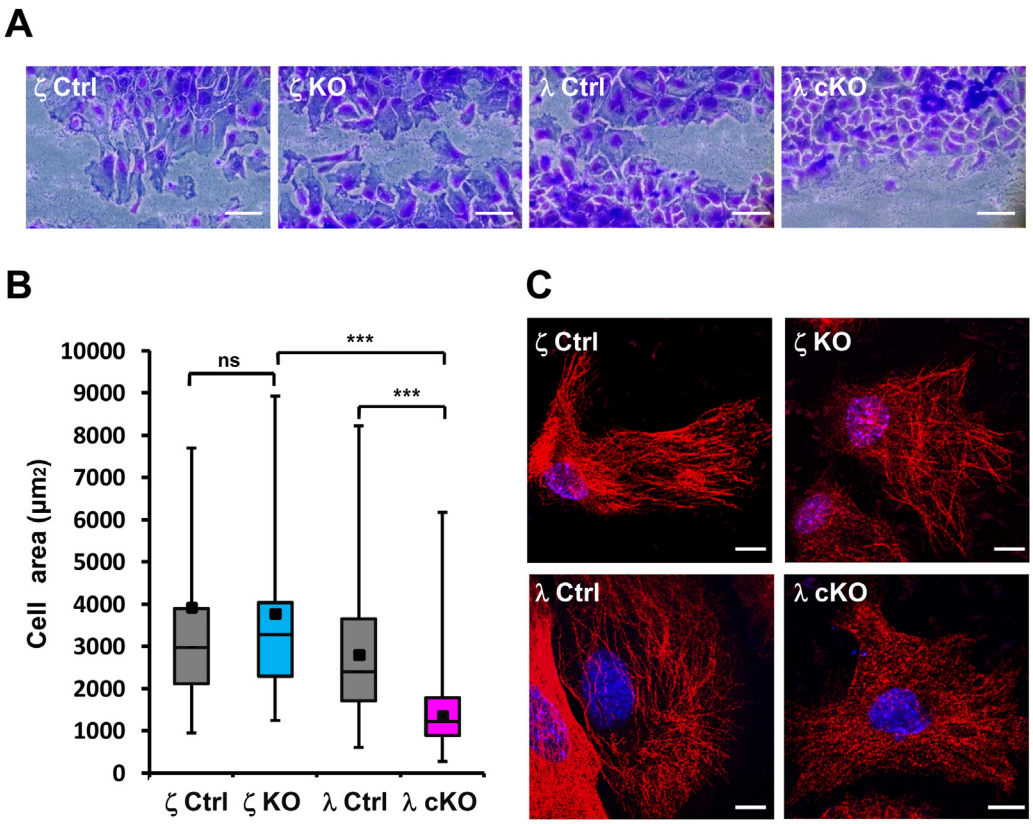

Fig. 5. Defects in microtubule extension in aPKCλ-deleted keratinocytes. (A) Closer views of wound-edge primary keratinocytes. Bar = 100 μm. (B) Box plot showing comparisons of the cell areas for wound-edge keratinocytes. The keratinocytes facing the wound were outlined using Image J software and the area of each cell was calculated. More than 150 cells per genotype were included. A black dot in each box plot denotes the mean value. $^{***}p < 0.001$. (C) Representative images of migrating keratinocytes facing the wound immunostained with an anti-β-tubulin antibody. Bar = 10 μm.

Our results that β-tubulin elongation was disrupted in aPKCλ-deleted, but not in aPKCζ-deleted keratinocytes, were inconsistent with the previous results that treatment of wild-type keratinocytes with a chemical aPKCζ inhibitor disrupted α-tubulin stabilization [18]. Moreover, the RNAi-based experiments in astrocytes, embryonic fibroblasts, and HeLa cells showed that aPKCζ plays an important role in cell migration. The differences in cell types, methods of gene inactivation and their specificities, and the proteins interacting with each aPKC isoform may account for this discrepancy.

Accumulating evidence indicates a role of the Wnt signaling pathway in cytoskeletal remodeling and cell motility. Wnt5a induces the Cdc42/Par6/aPKC complex [16] and the Dishevelled (Dvl)/Dishevelled-associating protein with a high frequency of leucine residues (Daple)/aPKC complex [29] to promote cell polarity and migration. In HEK293 T cells, aPKCλ, but not aPKCζ, associates with the Daple/Dvl complex [29]. Thus, it is possible that the destruction of the Daple/Dvl/aPKC complex as well as the Cdc42/Par/aPKC complex may also be involved in the randomized migration direction in aPKCλ-deleted keratinocytes. Consistent with our data, Daple deficiency was shown to impair epithelial cell migration in vivo during cutaneous wound healing [29].

Enough attention has not been paid to the functional differences between aPKCζ and aPKCλ. Here we show that aPKCs are not functionally equivalent; aPKCλ, but not aPKCζ, plays a primary role in cutaneous wound healing. Our results suggest that aPKCs differentially regulate a wide range of biological processes depending on the context.

Funding

None.

Conflict of interest

The authors have no conflict of interest to declare.

Acknowledgements

This work was supported by a Grant-in-Aid for Scientific Research (C) (#15K09755) from the Japan Society for the Promotion of Science to S.-I.O.

Appendix A. Supplementary data

Supplementary material related to this article can be found, in the online version, at doi:https://doi.org/10.1016/j.jdermsci.2019.01.001.

References

[1] J.A. Knoblich, Asymmetric cell division: recent developments and their implications for tumour biology, Nat. Rev. Mol. Cell Biol. 11 (2010) 849–860.
[2] A. Suzuki, S. Ohno, The PAR-aPKC system: lessons in polarity, J. Cell. Sci. 119 (2006) 979–987.
[3] S.E. Williams, S. Beronja, H.A. Pasolli, E. Fuchs, Asymmetric cell divisions promote Notch-dependent epidermal differentiation, Nature 470 (2011) 353–358.
[4] T. Lechler, E. Fuchs, Asymmetric cell divisions promote stratification and differentiation of mammalian skin, Nature 437 (2005) 275–280.
[5] I. Helfrich, A. Schmitz, P. Zigrino, C. Michels, I. Haase, A. le Bivic, et al., Role of aPKC isoforms and their binding partners Par3 and Par6 in epidermal barrier formation, J. Invest. Dermatol. 127 (2007) 782–791.
[6] M.T. Niessen, J. Scott, J.G. Zielinski, S. Vorhagen, P.A. Sotiropoulou, C. Blanpain, et al., aPKCλ controls epidermal homeostasis and stem cell fate through regulation of division orientation, J. Cell Biol. 202 (2013) 887–900.
[7] S.-I. Osada, N. Minematsu, F. Oda, K. Akimoto, S. Kawana, S. Ohno, Atypical protein kinase C isoform, aPKCλ, is essential for maintaining hair follicle stem cell quiescence, J. Invest. Dermatol. 135 (2015) 2584–2592.
[8] M. Takeo, W. Lee, M. Ito, Wound healing and skin regeneration, Cold Spring Harb. Perspect. Med. 5 (2015)a023267.
[9] M.V. Plikus, D.L. Gay, E. Treffeisen, A. Wang, R. June, G. Cotsarelis, et al., Epithelial stem cells and implications for wound repair, Semin. Cell Dev. Biol. 23 (2012) 946–953.
[10] M. Ito, Y. Liu, Z. Yang, J. Nguyen, F. Liang, R.J. Morris, et al., Stem cells in the hair follicle bulge contribute to wound repair but not to homeostasis of the epidermis, Nat. Med. 11 (2005) 1351–1354.
[11] V. Levy, C. Lindon, Y. Zheng, B.D. Harfe, B.A. Morgan, Epidermal stem cells arise from the hair follicle after wounding, FASEB J. 21 (2007) 1358–1366.
[12] H.J. Snippert, A. Haegebarth, M. Kasper, V. Jaks, J.H. van Es, N. Barker, et al., Lgr6 marks stem cells in the hair follicle that generate all cell lineages of the skin, Science 327 (2010) 1385–1389.
[13] I. Brownell, E. Guevara, C.B. Bai, C.A. Loomis, A.L. Joyner, Nerve-derived sonic hedgehog defines a niche for hair follicle stem cells capable of becoming epidermal stem cells, Cell Stem Cell 8 (2011) 552–565.
[14] M.E. Page, P. Lombard, F. Ng, B. Göttgens, K.B. Jensen, The epidermis comprises autonomous compartments maintained by distinct stem cell populations, Cell Stem Cell 13 (2013) 471–482.
[15] H. Xiao, M. Liu, Atypical protein kinase C in cell motility, Cell. Mol. Life Sci. 70 (2013) 3057–3066.
[16] K. Schlessinger, E.J. McManus, A. Hall, Cdc42 and noncanonical Wnt signal transduction pathways cooperate to promote cell polarity, J. Cell Biol. 178 (2007) 355–361.
[17] S. Etienne-Manneville, A. Hall, Integrin-mediated activation of Cdc42 controls cell polarity in migrating astrocytes through PKCζ, Cell 106 (2001) 489–498.
[18] S. Etienne-Manneville, A. Hall, Cdc42 regulates GSK-3β and adenomatous polyposis coli to control cell polarity, Nature 421 (2003) 753–756.
[19] D.M. Pegtel, S.I.J. Ellenbroek, A.E.E. Mertens, R.A. van der Kammen, J. de Rooij, J. G. Collard, The Par-Tiam1 complex controls persistent migration by stabilizing microtubule-dependent front-rear polarity, Curr. Biol. 17 (2007) 1623–1634.
[20] M. Leitges, L. Sanz, P. Martin, A. Duran, U. Braun, J.F. García, et al., Targeted disruption of the zetaPKC gene results in the impairment of the NF-κB pathway, Mol. Cell 8 (2001) 771–780.
[21] Y. Hirate, S. Hirahara, K.I. Inoue, A. Suzuki, V.B. Alarcon, K. Akimoto, et al., Polarity-dependent distribution of angiomotin localizes hippo signaling in preimplantation embryos, Curr. Biol. 23 (2013) 1181–1194.
[22] C.D. Nobes, A. Hall, Rho GTPases control polarity, protrusion, and adhesion during cell movement, J. Cell Biol. 144 (1999) 1235–1244.
[23] K.J. Hamill, S. Hiroyasu, Z.T. Colburn, R.V. Ventrella, S.B. Hopkinson, O. Skalli, et al., Alpha Actinin-1 regulates cell-matrix adhesion organization in keratinocytes: consequences for skin cell motility, J. Invest. Dermatol. 135 (2015) 1043–1052.
[24] S. Yamaji, A. Suzuki, H. Kanamori, W. Mishima, R. Yoshimi, H. Takasaki, et al., Affixin interacts with α-actinin and mediates integrin signaling for reorganization of F-actin induced by initial cell-substrate interaction, J. Cell Biol. 165 (2004) 539–551.
[25] T. Nishimura, K. Kaibuchi, Numb controls integrin endocytosis for directional cell migration with aPKC and PAR-3, Dev. Cell 13 (2007) 15–28.
[26] D. Bilder, M. Schober, N. Perrimon, Integrated activity of PDZ protein complexes regulates epithelial polarity, Nat. Cell Biol. 5 (2003) 53–58.
[27] T. Hirose, Y. Izumi, Y. Nagashima, Y. Tamai-Nagai, H. Kurihara, T. Sakai, et al., Involvement of ASIP/PAR-3 in the promotion of epithelial tight junction formation, J. Cell. Sci. 115 (2002) 2485–2495.
[28] K. Sasaki, T. Kakuwa, K. Akimoto, H. Koga, S. Ohno, Regulation of epithelial cell polarity by PAR-3 depends on Girdin transcription and Girdin-G i3 signaling, J. Cell. Sci. 128 (2015) 2244–2258.
[29] M. Ishida-Takagishi, A. Enomoto, N. Asai, K. Ushida, T. Watanabe, T. Hashimoto, et al., The Dishevelled-associating protein Daple controls the non-canonical Wnt/Rac pathway and cell motility, Nat. Commun. 3 (2012) 859.